Strain-induced band-gap engineering of graphene monoxide and its effect on graphene

H. H. Pu,[1] S. H. Rhim,[2] C. J. Hirschmugl,[2] M. Gajdardziska-Josifovska,[2] M. Weinert,[2,*] and J. H. Chen[1,†]

[1]*Department of Mechanical Engineering and Laboratory for Surface Studies, University of Wisconsin-Milwaukee, Milwaukee, Wisconsin 53211, USA*

[2]*Department of Physics and Laboratory for Surface Studies, University of Wisconsin-Milwaukee, Milwaukee, Wisconsin 53211, USA*

(Received 24 October 2012; published 13 February 2013)

Using first-principles calculations we demonstrate the feasibility of band-gap engineering in two-dimensional crystalline graphene monoxide (GMO), a recently reported graphene-based material with a 1:1 carbon/oxygen ratio. The band gap of GMO, which can be switched between direct and indirect, is tunable over a large range (0–1.35 eV) for accessible strains. Electron and hole transport occurs predominantly along the zigzag and armchair directions (armchair for both) when GMO is a direct- (indirect-) gap semiconductor. A band gap of ∼0.5 eV is also induced in graphene at the K' points for GMO/graphene hybrid systems.

DOI: 10.1103/PhysRevB.87.085417 PACS number(s): 73.61.−r, 68.35.Gy, 72.80.Le

I. INTRODUCTION

Graphene has sparked intense research interest among various scientific communities since its experimental isolation via mechanical exfoliation in 2004.[1] Due to its superior electron mobility (∼200 000 cm^2/V s at room temperature[2]), graphene has been envisioned as a replacement for silicon in digital logic circuits, but its semimetallic nature severely limits its use in semiconductor applications. Although graphene-based transistors with a cutoff frequency as high as 300 GHz (Ref. 3) have been achieved, the poor on/off ratio of ∼1000 at room temperature[4,5] is still far away from that (>10 000) of silicon transistors.[6] Significant effort has been devoted to identifying mechanisms to tailor the energy band gap of graphene, including application of a gate voltage,[7] interactions with substrates,[8,9] and the formation of nanoribbons,[10] graphene nanomeshes,[11] and graphene quantum dots[12] nanostructures. A band gap of 0.25 eV has been reported for bilayer graphene[7] through the gating effect, and monolayer graphene grown epitaxially on SiC substrates produces a similar band gap (∼0.26 eV).[8,9] Armchair graphene nanoribbons (AGNR) achieve band gaps around 1 eV for widths below ∼1.5 nm,[13,14] but with considerable degradation of electron mobility.[15] Moreover, variations in the band gap are inevitable due to inherent edge disorder,[14] which is also true for graphene nanomeshes and quantum dots. Since precision control of the edge type and its purity is a prerequisite for GNR-based nanoelectronics, the successful introduction of the next generation of electronic devices based on graphene requires new approaches to efficiently engineer the band gap.

Recently a new graphene-based structure, graphene monoxide (GMO), has been reported based on electron diffraction observations during *in situ* thermal reduction of multilayer graphene oxide (GO) under vacuum in a transmission electron microscope (TEM) chamber.[16] Supported by infrared spectroscopy and first-principles calculations, the new two-dimensional material was identified as a two-phase hybrid containing GMO domains that evolve in the graphene matrix. The resulting GMO is crystalline—in a quasihexagonal/centered-rectangular lattice—with the two C atoms in the graphene unit cell bridged by two O atoms to form a double epoxy structure with a concomitant ∼20% increase in the planar cell area. Moreover, GMO has a higher oxygen to carbon ratio (O:C = 1:1) than unreduced GO, which varies from $C_1O_{0.5}$ to $C_1O_{0.75}$[17–19] and is predicted to be insulating.[17] In contrast, GMO has been predicted to be semiconducting.[16,20]

Of the many efforts devoted to identifying potential mechanisms for generating band gaps in graphene and related materials, few can be used to tune the band gap over a wide range on the same device. In this paper we use first-principles calculations to explore the interplay between the mechanical and electronic properties of pure GMO and its one-dimensional interface with graphene. The results show that GMO is mechanically soft compared with graphene, and that strain can alter the magnitude of the band gap by more than 1 eV, changing GMO from an indirect- to a direct-gap semiconductor (IGMO to DGMO), or even into a metallic state. The rich electronic landscape of strained GMO is accompanied by potentially useful changes in carrier mobility and anisotropy. Furthermore, GMO is found to induce a direct band gap of ∼0.5 eV in graphene, extending more than 15 Å from the interface between GMO and graphene. The ability to tune the band gap by application of strains in the GMO region and the intrinsic two-dimensional semiconducting nature of GMO opens new opportunities for developing graphene-based electronics.

II. MODEL AND METHODS

The calculations were done using the full-potential linearized augmented plane wave (FLAPW) method as implemented in *flair*.[21] A plane wave cutoff of 275 eV was used for the expansion of the wave functions, the Brillouin zone was sampled using a 12 × 12 × 1 mesh, and the generalized gradient approximation (GGA) for exchange-correlation was used. Figure 1(a) shows the crystalline structure of GMO. Each C atom forms four bonds, two along the zigzag direction to the neighboring C atoms, and two with the bridging O atoms along the armchair direction. The two-dimensional centered-rectangular (quasihexagonal) structure can be described by two of three interrelated parameters: the length of the rhombus edge a_o, the opening angle α (equal to 120° for hexagonal systems), and the width of the conventional rectangular cell [$d_{O\text{-}O}$ in Fig. 1(a)]. The internal atomic positions of all the

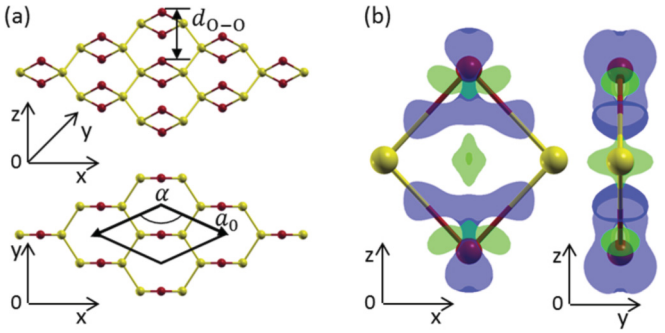

FIG. 1. (Color online) Structure and difference charge density of GMO. (a) Perspective and top views of GMO in a 3 × 3 cell with lattice parameters labeled. C (O) atoms are represented by yellow (red) balls; all C atoms are in the same plane. (b) Side views of the difference between the self-consistent and overlapping atomic electron densities ($\triangle n = n_{CO} - n_C - n_O$) of GMO. Light blue and green isosurfaces ($\pm 0.05\, e/a_B{}^3$) indicate accumulation and depletion of electrons, respectively.

atoms were fully relaxed (3×10^{-3} eV/Å) for each set of parameters.

III. RESULTS AND DISCUSSION

A. Atomic and electronic structure of GMO

For the fully relaxed ground state structure ($a_0 = 3.10$ Å, $\alpha = 130°$), the C-C bond length (1.56 Å) is close to typical values (~1.54 Å) of C sp^3 bonds, while the C-O bond length (1.43 Å) is comparable to sp^2 C-C bonds (1.42 Å). Since the stiffness of graphene is strongly dependent on the planar sp^2 σ bonds, the large C-C bond lengths compared with graphene suggest (and borne out by the calculations) that GMO is less rigid than graphene. The higher electronegativity[22] of O (3.44) than that of C (2.55) is consistent with the calculated result [cf. Fig. 1(b)] that electrons accumulate near the C-O bonds and the O atoms.

The calculated trends in the distortion energies of GMO as a function of α and $d_{O\text{-}O}$ are given in Fig. 2(a). The

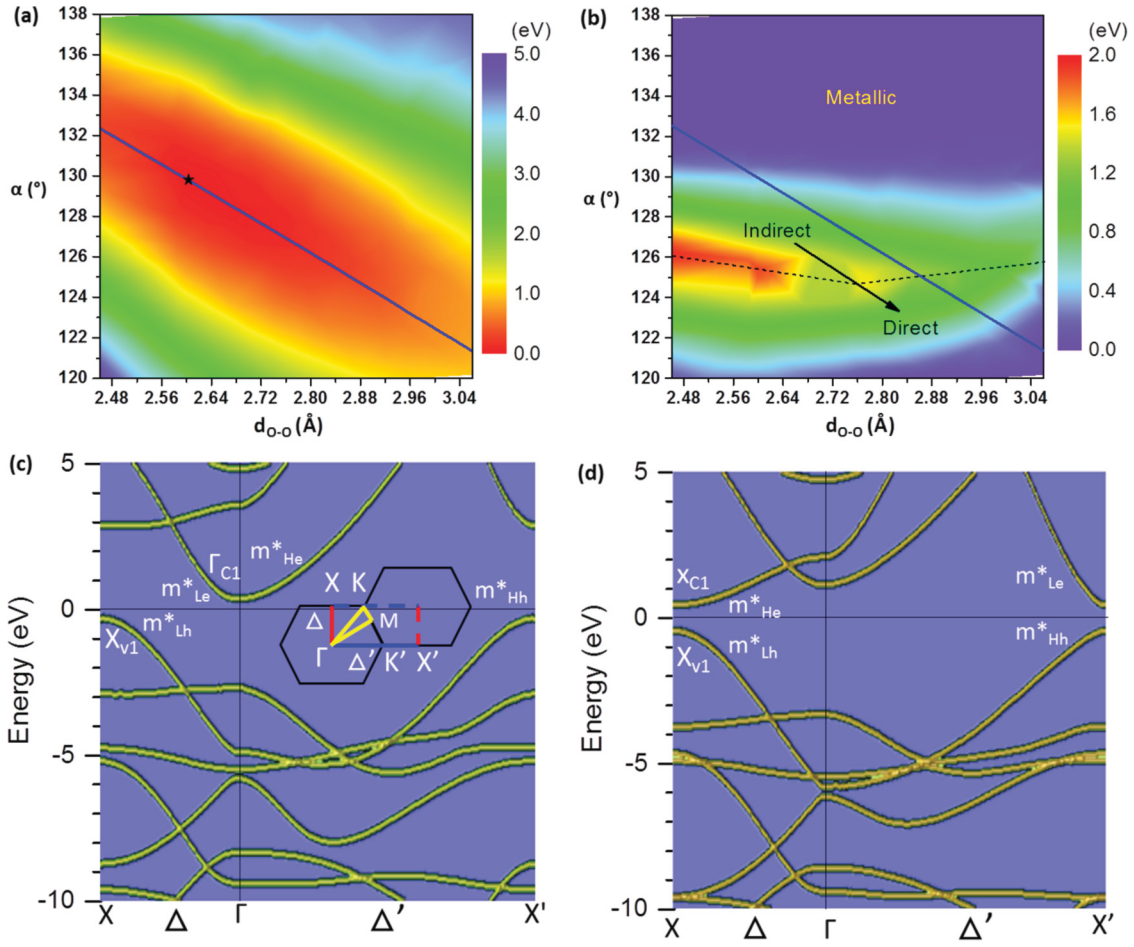

FIG. 2. (Color online) (a) Distortion energies relative to the fully relaxed GMO structure per CO formula unit as functions of the structural parameters α and $d_{O\text{-}O}$ given in Fig. 1(a). The black star represents the lattice parameters of the fully relaxed structure; the blue line indicates a constant $a_0 = 3.10$ Å. (b) Calculated band gap of GMO as a function of α and $d_{O\text{-}O}$. The calculated crossover between direct and indirect gap is indicated by the dashed line. Calculated bands for $a_0 = 3.10$ Å in (c) $\alpha = 130°$ and (d) $\alpha = 125°$. The inset in (c) shows the symmetry lines and points in the Brillouin zone for GMO. Since the point group symmetry of GMO is D_{2h}, compared with the D_{6h} symmetry of graphene, the K' point in GMO has no additional symmetry compared to other points along Δ'. The effective mass labels indicate light and. heavy electrons (m^*_{Le}, m^*_{He}) and holes (m^*_{Lh}, m^*_{Hh}).

energy cost for rather large distortions is small, and the "energy valley" is approximately aligned along constant a_o (=3.10 Å). External strains are accommodated mainly by changes in α (or equivalently, $d_{O\text{-}O}$) rather than by changes in a_o: The low-energy structure has a modulus of ~570 GPa along the zigzag direction, about half of the graphene modulus (~1.1 TPa)[23]. Figure 2(b) presents the calculated band gaps corresponding to the structure parameters in Fig. 2(a). (Although the gaps are likely underestimated, as common in DFT calculations, the trends and overall band topologies are expected to be valid.) For the fully optimized structure, GMO is a semiconductor with a calculated indirect band gap of ~0.6 eV. Upon planar deformation, GMO spans the range of semiconducting (both indirect and direct gap) and metallic behaviors. Stretching along the zigzag direction (increasing d_{O-O}), causes the band gap of GMO to vary from ~0.6 eV (indirect gap, at 130°) up to ~1.4 eV (both indirect and direct gap, at 126°), then down to ~0.1 eV (direct gap, at 121°). The sensitive response of the band gap to external strains in GMO could be attractive for low-cost fabrication of building blocks in nanoelectromechanical systems (NEMS). In contrast, graphene is not an ideal candidate for NEMS since the electronic structure of graphene is robust against external strains up to ~23%,[24] while the fracture strain is ~25%.[25] Although the band gap of GNR with armchair edges has been theoretically predicted to be tunable by mechanical perturbations and may have a semiconductor-metal transition as the strain increases,[26] the uniaxial modulus of these GNRs is extremely large, ~7 TPa,[27] imposing severe constraints for practical NEMS applications.

To tailor the semiconducting behavior of the graphene-based materials, it is necessary to understand the origin of the states around the Fermi level. Representative band structures, for the same a_o, but different angles α, are shown in Figs. 2(c) and 2(d). The low-lying conduction bands exhibit large variations, while the valence bands have small changes, as α varies from 130° to 125°: The conduction band state labeled Γ_{C1} (X_{C1}) undergoes an upward (downward) shift of ~0.8 eV (2.6 eV), while X_{V1} moves down ~0.1 eV. Such band shifts are indicative of significant changes in the interactions between atomic orbitals on different sites with respect to angle α for a fixed lattice constant a_o. Figures 3(a)–3(d) present the charge density distributions corresponding to the states at the top and the bottom of the gap, as labeled in Figs. 2(c) and 2(d). The conduction band edge states (Γ_{C1} and X_{C1}) exhibit different character, with X_{C1} having no O $2p$ contributions. On the C atoms, the conduction states are predominantly p_z for Γ_{C1} (IGMO), whereas for X_{C1} (DGMO) there is a strong admixture of p_x. Since the C p_x-p_x interaction varies as $l^2 V_{pp\sigma} + (1 - l^2)V_{pp\pi}$, where l is the direction cosine and $V_{pp\sigma}$, $V_{pp\pi}$ are Koster-Slater tight-binding parameters, the energy of the X_{C1} state in particular changes significantly with α, as seen in Figs. 2(c) and 2(d). The gap edge valence state X_{V1}, on the other hand, is predominantly O p_y (with small admixture of p_z) and bonding C sp^2 (p_x,p_y) orbitals that would form a conduction network along the zigzag direction for p-doped GMO.

The band gap (width and type) and the charge carrier mobility—which is inversely proportional to its effective mass—are critical features for semiconductor-based device

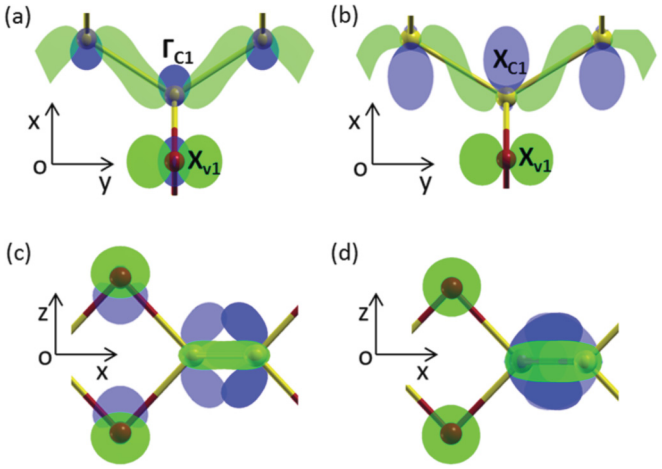

FIG. 3. (Color online) Charge density isosurfaces (0.05 $e/a_B{}^3$) of states at the top of the valence band (light green) and at the bottom of the conduction band (blue) in top and side views. (a) and (c) IGMO: Γ_{C1} and X_{V1} [cf. Fig. 3(a)]; (b) and (d) DGMO: X_{C1} and X_{V1} [cf. Fig. 3(b)].

applications. As shown above, GMO may be either a direct or indirect band-gap semiconductor, and has a tunable band gap. As a measure of the transport properties, Fig. 4 shows the effective masses for electrons and holes as a function of the angle α. The electron effective masses change dramatically when GMO is switched from indirect- to direct-gap semiconductor as a result of the conduction band minimum changing from Γ to X. The hole mass along the armchair direction (X to Γ) remains fairly constant, but there is an increase along the zigzag direction with decreasing α. In the case of IGMO, the light electrons (preferred conduction) are along the armchair direction, i.e., through the C-O-C double epoxy units; in the case of DGMO, the light electrons are in the zigzag direction through the · · ·-C-C-C-· · · network. For the holes, the

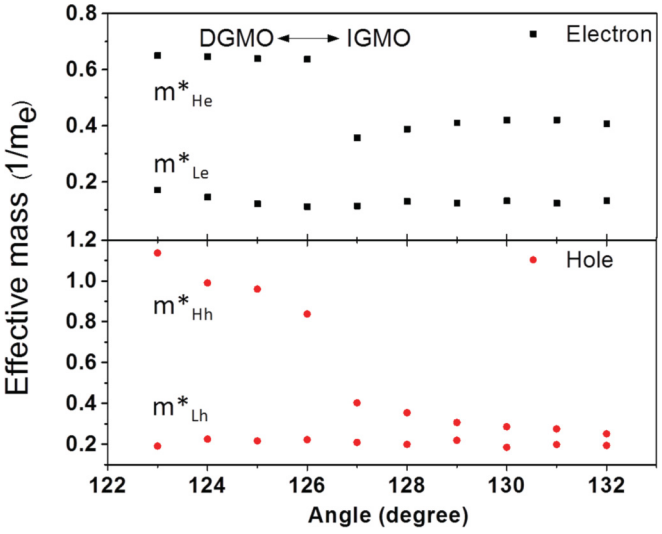

FIG. 4. (Color online) Electron (black squares) and hole (red circles) effective masses are shown for anisotropic GMO. The effective masses of carriers with respect to lattice angles are evaluated from quadratic fits to the band dispersion. The transition from IGMO to DGMO is ~126°.

preferred conduction is along the armchair direction for both IGMO and DGMO. The calculated GMO effective masses ($m^*_{Le}/m_e = 0.112$–$0.132, m^*_{Lh}/m_e = 0.185$–$0.225$) are larger than those in Ge ($m^*_{Le}/m_e = 0.041$, $m^*_{Lh}/m_e = 0.044$) and group III-V semiconductors ($m^*_{Le}/m_e = 0.015$–0.11, $m^*_{Lh}/m_e = 0.021$–0.082),[28] but they are comparable to those of Si ($m^*_{Le}/m_e = 0.20$, $m^*_{Lh}/m_e = 0.15$)[29] and GNR with similar band gaps ($m^*_{Le}/m_e = m^*_{Lh}/m_e = 0.075$–$0.10$ for band gaps of 0.2–0.5 eV, with the effective mass drastically increasing above 0.1 when the band gap exceeds 0.5 eV[15]).

B. GMO-graphene interface

GMO as originally observed[16] is likely embedded within a graphene matrix; moreover, if GMO is to be incorporated into graphene-based nanoelectronics, understanding the interface between the two materials is essential. To investigate how the interface affects the electronic structure of both graphene and GMO, we consider a simplified model of the combined system consisting of a periodic array of ∼30 Å stripes of both graphene and GMO, with the interface along the zigzag direction and with d_{O-O} of GMO fixed to the corresponding distance in graphene [Fig. 5(a)], thus the atoms in the GMO region are relaxed only along the armchair direction; at this $d_{O\text{-}O}$ GMO is metallic [cf. Fig. 2(b)]. Although a realistic modeling of the device characteristics of a GMO-graphene hybrid would require far larger cells and the inclusion of disorder, further interface relaxations, and beyond DFT/GGA corrections to the energy bands, the results illustrate the basic effects that will occur at such an interface. Energetically there is a cost related to this distortion of the GMO, but the formation of GMO is still energetically more favorable (by ∼0.2 eV/O atom in our calculations) than forming isolated epoxide groups[20] or carbonyl pairs, which are the most stable functional groups in graphene oxide.[30]

Figure 5(b) shows the (local) band structure of the combined system in the middle of the graphene region and k-projected ("unfolded") onto the graphene 1 × 1 Brillouin zone. In contrast to graphene, there is a band gap of ∼0.5 eV at the K' point—Γ-K'-M corresponding to propagation along the graphene ribbon—with almost linear dispersion, as shown in the inset. (The bands at the nominally equivalent K' and K points for pristine graphene are different here.) This induced gap is significantly larger than the gap of ∼0.2 eV expected for zigzag GNRs of the same width,[14] pointing out the influence of the graphene-GMO interface. Figure 5(c) shows the local k-projected band structure of the GMO region. The electronic states from graphene extend throughout the ∼30 Å wide GMO region: Although in pure GMO (cf. Fig. 2), there are no states within several eV of the Fermi level at K', images of the graphene bands in Fig. 5(b) are clearly seen along Γ-K'-X' in Fig. 5(c). The gap at K' in the graphene region has increased (doubled) to ∼1 eV in the GMO region of the composite. (The bands around K' display aspects of being at a high symmetry point, which is true for pure graphene, but not GMO, further evidence of the leakage of graphene states.) Similarly, there are remnants of the GMO bands in the graphene region, i.e., there is a complicated superimposition and entanglement of graphene and GMO states near the interface. The effects of the lateral confinement and interaction effects due to the finite widths of the ribbons are particularly noticeable along X-Γ (and M-Γ of the graphene) since this is the direction corresponding to propagation across the interface. In the GMO region there are two sets of bands that form a staircase of

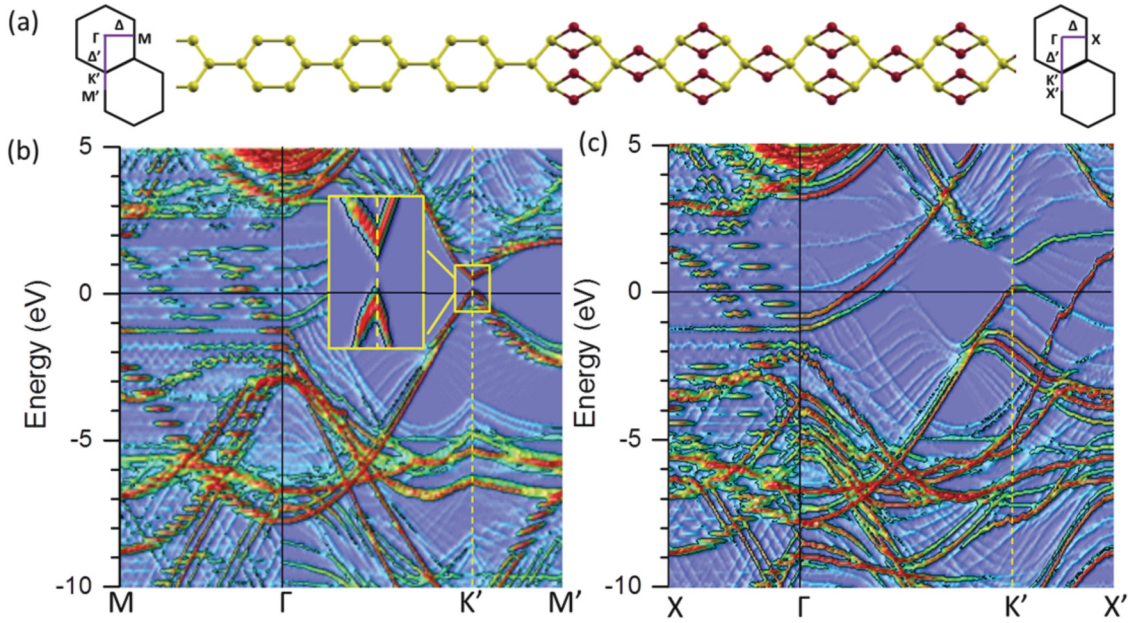

FIG. 5. (Color online) (a) Interface model of graphene and GMO with $d_{O\text{-}O}$ [cf. Fig. 1(a)] fixed to the lattice constant of graphene (2.46 Å). The 1 × 1 Brillouin zones with labels for the graphene and GMO regions are indicated. (b) and (c) k-projected band structures for graphene and GMO, respectively, in the middle of each region. The inset in (b) is a magnified view of the bands around K' enclosed in the yellow rectangle. (The k projection decomposes the supercell wave functions into momentum components of the 1 × 1 cells, thus "unfolding" the bands; the resulting states are then spatially integrated to give the relative intensities—varying from blue to red—shown.)

states with fairly well-defined momenta and energies. These bands corresponding to those shown in Figs. 3(a) and 3(c); note that the other bands do not show the same staircase behavior, indicating that the origin of the staircases is not simply confined to the GMO ribbon. These GMO states, in fact, extend into the graphene, being the dominant states along M-Γ within a few eV of the Fermi level [Fig. 5(b)].

To further explore the tunable electronic properties of GMO by small external mechanical strain, we investigated the effect of uniform compressive strain along the armchair direction of GMO assuming that the hexagonal symmetry of graphene is maintained due to the large difference of Young's moduli.[31] For a compressive strain of $\sim -2.5\%$, GMO is still metallic and the band structure of graphene maintains the same features, except the graphene band gap decreases to $\sim$0.4 eV. If the strain is increased to -3.5%, however, the band gap of graphene increases to $\sim$0.6 eV and GMO becomes semiconducting; therefore, GMO might also be used as a tool to tune the band gap in graphene at the G-GMO interface. These types of strains could potentially be realized in GMO—piezoelectric/ferroelectric nanostructure devices, allowing the active real-time modification of the band gap.

IV. CONCLUSIONS

First-principles calculations were presented to elucidate the structural, mechanical, and electronic properties of the newly discovered GMO, whose two-dimensional crystalline form offers great potential for future electronic applications. The band gap of GMO is found to be sensitive to the lattice angle (120°–134°) and varies between 0 to over 1.3 eV, with the nature of the band gap switching from direct to indirect as the lattice angle increases. The distinctive characteristics of direct- and indirect-gap GMO semiconductors arise from their sensitive electronic response to external mechanical strains. The strong anisotropic nature of DGMO causes electrons and holes to preferentially move along the zigzag and armchair directions, respectively, minimizing the rate of recombination between electrons and holes, a desirable feature for photovoltaic devices. The band-gap opening and quasilinear band dispersion in the graphene region near the G-GMO interface suggest the G-GMO structures could find potential applications in future semiconductor devices. Finally, the O atoms in GMO could act as adsorption sites for various adsorbates (e.g., gas molecules, metal ions such as lithium ions, and metal-organic complexes), making GMO a potential candidate for applications in sensors and lithium-ion battery electrodes.

ACKNOWLEDGMENTS

The authors acknowledge the financial support from the National Science Foundation (CMMI-0856753 and CMMI-0900509), and from the Research Growth Initiative Program of the University of Wisconsin-Milwaukee (UWM).

*Corresponding author: weinert@uwm.edu
†Corresponding author: jhchen@uwm.edu

[1] K. S. Novoselov, A. K. Geim, S. V. Morozov, D. Jiang, Y. Zhang, S. V. Dubonos, I. V. Grigorieva, and A. A. Firsov, Science **306**, 666 (2004).
[2] K. I. Bolotin, K. J. Sikes, Z. Jiang, M. Klima, G. Fudenberg, J. Hone, P. Kim, and H. L. Stormer, Solid State Commun. **146**, 351 (2008).
[3] L. Liao, Y.-C. Lin, M. Bao, R. Cheng, J. Bai, Y. Liu, Y. Qu, K. L. Wang, Y. Huang, and X. Duan, Nature (London) **467**, 305 (2010).
[4] Y. Lu, B. Goldsmith, D. R. Strachan, J. H. Lim, Z. Luo, and A. T. C. Johnson, Small **6**, 2748 (2010).
[5] F. Xia, D. B. Farmer, Y.-m. Lin, and P. Avouris, Nano Lett. **10**, 715 (2010).
[6] M. A. Rafiq, K. Masubuchi, Z. A. K. Durrani, A. Colli, H. Mizuta, W. I. Milne, and S. Oda, Appl. Phys. Lett. **100**, 113108 (2012).
[7] Y. Zhang, T.-T. Tang, C. Girit, Z. Hao, M. C. Martin, A. Zettl, M. F. Crommie, Y. R. Shen, and F. Wang, Nature (London) **459**, 820 (2009).
[8] Y. Qi, S. H. Rhim, G. F. Sun, M. Weinert, and L. Li, Phys. Rev. Lett. **105**, 085502 (2010).
[9] S. Y. Zhou, G. H. Gweon, A. V. Fedorov, P. N. First, W. A. De Heer, D. H. Lee, F. Guinea, A. H. C. Neto, and A. Lanzara, Nat. Mater. **6**, 770 (2007).
[10] L. C. Campos, V. R. Manfrinato, J. D. Sanchez-Yamagishi, J. Kong, and P. Jarillo-Herrero, Nano Lett. **9**, 2600 (2009).
[11] X. Liang, Y.-S. Jung, S. Wu, A. Ismach, D. L. Olynick, S. Cabrini, and J. Bokor, Nano Lett. **10**, 2454 (2010).
[12] L. A. Ponomarenko, F. Schedin, M. I. Katsnelson, R. Yang, E. W. Hill, K. S. Novoselov, and A. K. Geim, Science **320**, 356 (2008).
[13] M. Y. Han, B. Ozyilmaz, Y. Zhang, and P. Kim, Phys. Rev. Lett. **98**, 206805 (2007).
[14] Y.-W. Son, M. L. Cohen, and S. G. Louie, Phys. Rev. Lett. **97**, 216803 (2006).
[15] E. Sano and T. Otsuji, Jpn. J. Appl. Phys. **48**, 041202 (2009).
[16] E. C. Mattson, H. Pu, S. Cui, M. A. Schofield, S. Rhim, G. Lu, M. J. Nasse, R. S. Ruoff, M. Weinert, M. Gajdardziska-Josifovska, J. Chen, and C. J. Hirschmugl, ACS Nano **5**, 9710 (2011).
[17] D. W. Boukhvalov and M. I. Katsnelson, J. Am. Chem. Soc. **130**, 10697 (2008).
[18] S. Mao, H. Pu, and J. Chen, Rsc. Adv. **2**, 2643 (2012).
[19] T. Szabo, O. Berkesi, P. Forgo, K. Josepovits, Y. Sanakis, D. Petridis, and I. Dekany, Chem. Mater. **18**, 2740 (2006).
[20] H. J. Xiang, S.-H. Wei, and X. G. Gong, Phys. Rev. B **82**, 035416 (2010).
[21] M. Weinert, G. Schneider, R. Podloucky, and J. Redinger, J. Phys.: Condens. Matter **21**, 084201 (2009).
[22] A. L. Allred, J. Inorg. Nucl. Chem. **17**, 215 (1961).
[23] C. Lee, X. Wei, J. W. Kysar, and J. Hone, Science **321**, 385 (2008).
[24] V. M. Pereira, A. H. Castro Neto, and N. M. R. Peres, Phys. Rev. B **80**, 045401 (2009).

[25]F. Liu, P. Ming, and J. Li, Phys. Rev. B **76**, 064120 (2007).
[26]M. Poetschke, C. G. Rocha, L. E. F. Foa Torres, S. Roche, and G. Cuniberti, Phys. Rev. B **81**, 193404 (2010).
[27]O. Hod and G. E. Scuseria, Nano Lett. **9**, 2619 (2009).
[28]M. C. Peter and Y. Yu, *Fundamentals of Semiconductors: Physics and Materials Properties* (Springer, Berlin, 1999).
[29]T. B. Boykin, G. Klimeck, and F. Oyafuso, Phys. Rev. B **69**, 115201 (2004).
[30]M. Acik, G. Lee, C. Mattevi, M. Chhowalla, K. Cho, and Y. J. Chabal, Nat. Mater. **9**, 840 (2010).

[31]The Young's moduli for GMO and graphene along the zigzag direction are ∼0.6 and ∼1.1 GPa, respectively. A 2.5% (3.5%) strain changes the angle of GMO from 133.0° to 132.1° (131.7°) at an energy cost of ∼60 meV (80 meV); for graphene, the corresponding distortion is 0.5°. In realistic systems, dislocations, rather than uniform expansions/contractions, will form to relieve the strain at the interface. Because of the difference in bonding of GMO vs graphene, dislocations are more likely in GMO. Thus, while the graphene at the interface will be strained, the resulting distortions are expected to be much smaller than in GMO.